Energy Materials

Supplementary Materials

Bilateral coordination interfaces enable long-term stable organic solar cells under multiple stress conditions

Nurul Kusuma Wardani[1,2], Muhammad Jahandar[1], Yong Hyun Kim[2], Soyeon Kim[1], Dong Chan Lim[1]

[1]Energy and Environment Materials Research Division, Korea Institute of Materials Science (KIMS), Changwon 51508, Republic of Korea.

[2]Department of Smart Green Technology Engineering, Pukyong National University, Busan 48513, Republic of Korea.

Correspondence to: Dr. Soyeon Kim, Dr. Dong Chan Lim, Energy and Environment Materials Research Division, Korea Institute of Materials Science (KIMS), Changwon 51508, Republic of Korea. E-mail: kimso1965@kims.re.kr; dclim@kims.re.kr

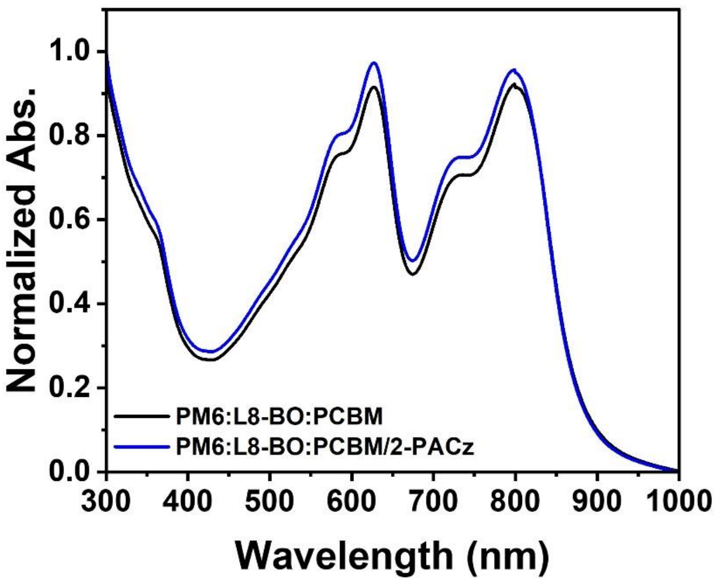

Supplementary Figure 1: Normalized absorbance spectra of BHJ layer and BHJ/2PACz

Supplementary Table 1: Work function values of pristine and interlayer-modified ITO electrodes determined from UPS measurements.

ETL	Work function (eV)
ITO	-4.40
ITO/PDINN	-4.10
ITO/PDINN/BCP	-4.04
ITO/PDINN/Cu-BCP	-3.94

Supplementary Table 2: Summary of the electrical conductivity values for ITO/interlayer/Ag structures employing PDINN, PDINN/BCP, and PDINN/Cu-BCP interlayers.

ETL	Electrical conductivity (σ_0, $S.m^{-1}$)
ITO/PDINN/Ag	1.18×10^{-6}
ITO/PDINN/BCP/Ag	1.29×10^{-6}
ITO/PDINN/Cu-BCP/Ag	1.50×10^{-6}

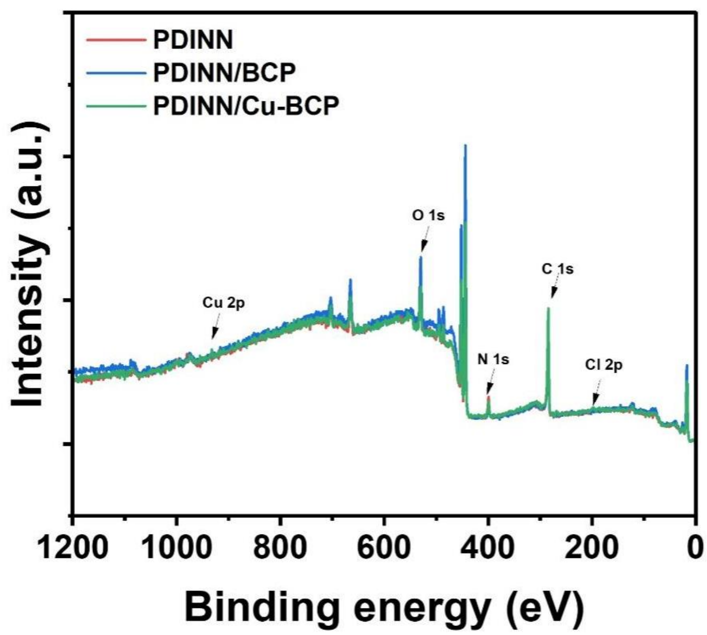

Supplementary Figure 2: Full spectra of ITO/PDINN; ITO/PDINN/BCP; ITO/PDINN/Cu-BCP

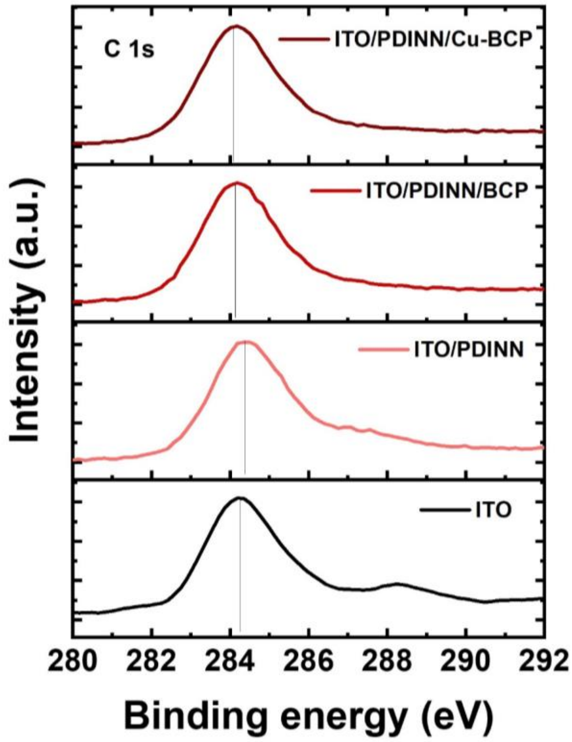

Supplementary Figure 3: High-resolution C 1s XPS spectra of pristine ITO and ITO modified with PDINN, PDINN/BCP, and PDINN/Cu-BCP interlayers.

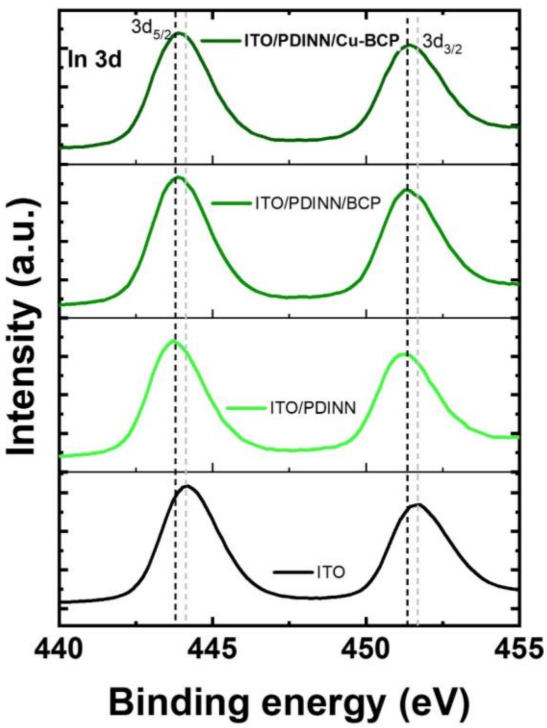

Supplementary Figure 4: High-resolution In 3d XPS spectra of pristine ITO and ITO modified with PDINN, PDINN/BCP, and PDINN/Cu-BCP interlayers

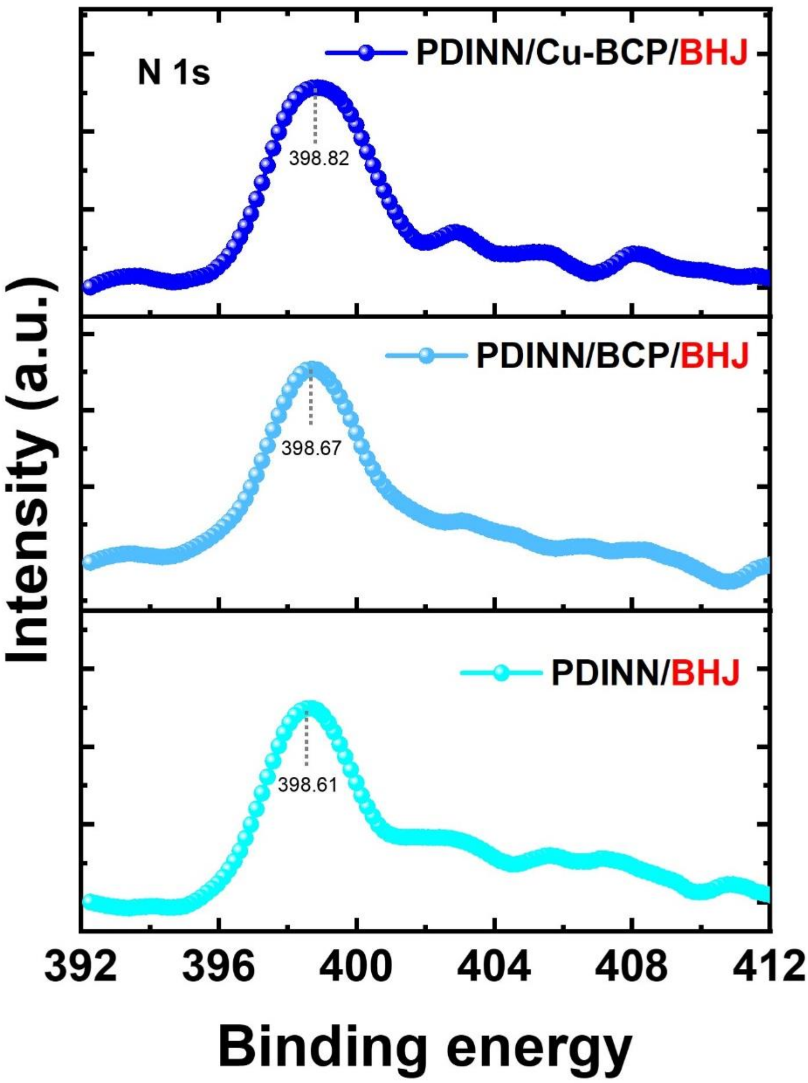

Supplementary Figure 5: High-resolution N 1s XPS spectra of PDINN, PDINN/BCP, and PDINN/Cu-BCP with BHJ

Supplementary Table 3: Summary of XPS core-level peak positions for ITO/PDINN, ITO/PDINN/BCP, and ITO/PDINN/Cu-BCP interlayer films.

Sample	N 1s BE (eV)	O 1s BE (eV)
ITO/PDINN	398.78	530.08
ITO/PDINN/BCP	399.05	529.62
ITO/PDINN/Cu-BCP	399.33	530.08

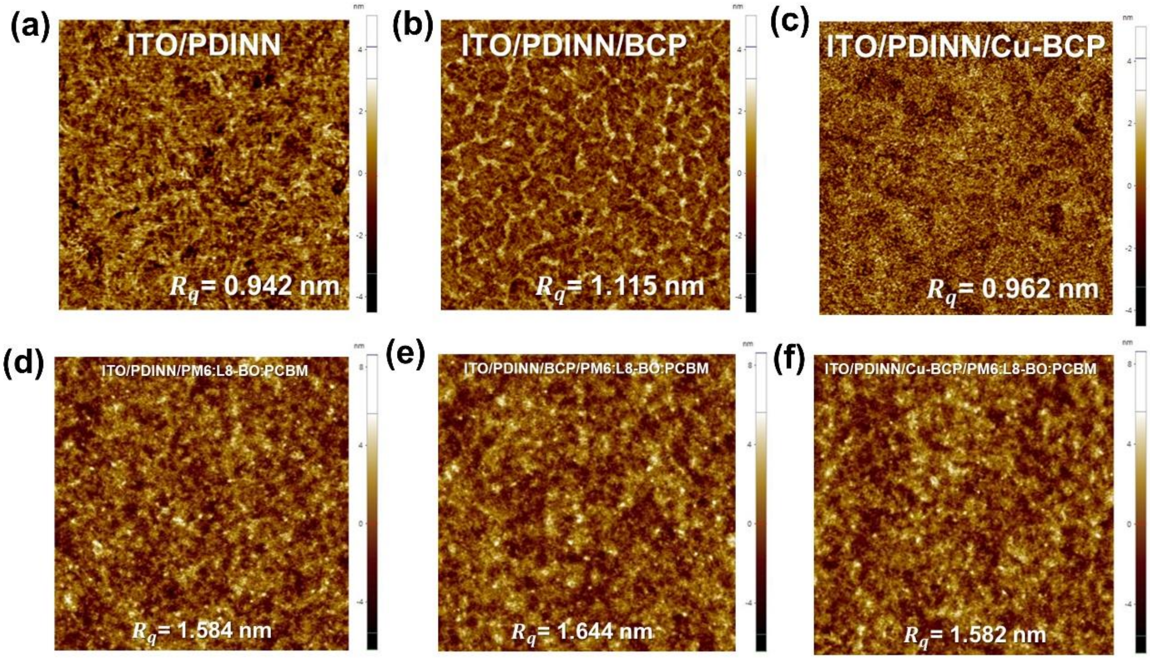

Supplementary Figure 6: Surface morphology of PDINN-based cathode interlayers and overlying bulk-heterojunction films. AFM height images of a: ITO/PDINN; b: ITO/PDINN/BCP; c: ITO/PDINN/Cu-BCP; d: ITO/PDINN/BHJ; e: ITO/PDINN/BCP/BHJ; f: ITO/PDINN/Cu-BCP/BHJ

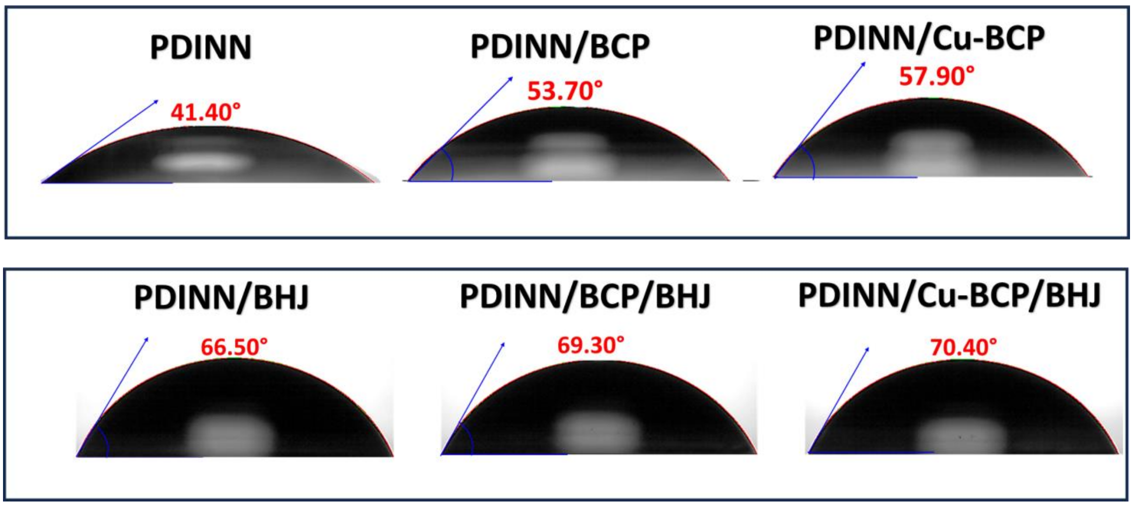

Supplementary Figure 7: Static water contact angle images of PDINN, PDINN/BCP, and PDINN/Cu-BCP interlayers (top), and the corresponding BHJ-coated films (PDINN/BHJ, PDINN/BCP/BHJ, and PDINN/Cu-BCP/BHJ) (bottom)

Supplementary Table 4. Comparison of device performance parameters of inverted OSC based on PM6:L8-BO:$PC_{71}BM$ photoactive layer with various $CuCl_2$:BCP ratio with MoOx as HTL

$CuCl_2$:BCP (ratio)	**V_{OC} (V)**	**J_{SC} (mA/cm^2)**	**FF (%)**	**PCE (%)**
1 : 0.5	0.84	22.72	69.20	13.37
1 : 3	0.85	24.30	68.25	13.62
1 : 5	0.85	25.00	71.90	15.24
1 : 7	0.86	22.85	67.72	13.36

Supplementary Table 5: Comparison of device performance parameters of inverted OSC based on PM6:L8-BO:$PC_{71}BM$ photoactive layer with various CILs (PDINN, PDINN/BCP, and PDINN/Cu-BCP) with MoOx as HTL

CILs	**V_{OC} (V)**	**J_{SC} (mA/cm^2)**	**FF (%)**	**PCE (%)**
PDINN	0.82	24.19	69	13.69
PDINN/BCP	0.84	24.51	71	14.62
PDINN/Cu-BCP	0.85	24.53	73	15.30

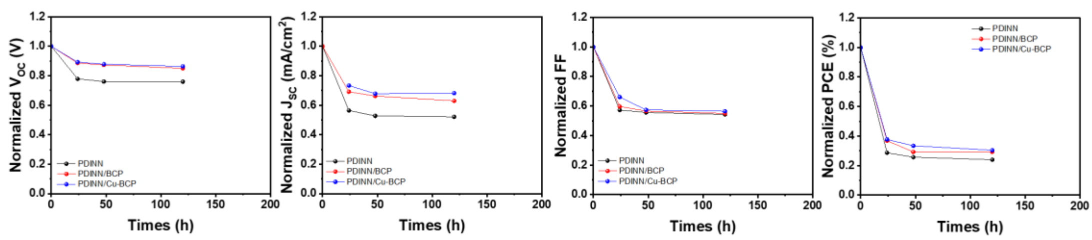

Supplementary Figure 8: Evolution of the normalized photovoltaic parameters of OSCs with different cathode interlayers during aging: normalized V_{OC}, normalized J_{SC}, normalized FF and normalized PCE during continuous 1-sun photo-illumination (25°C/25%RH) aging for PDINN, PDINN/BCP, and PDINN/Cu-BCP devices with MoOx as HTLs (encapsulation).

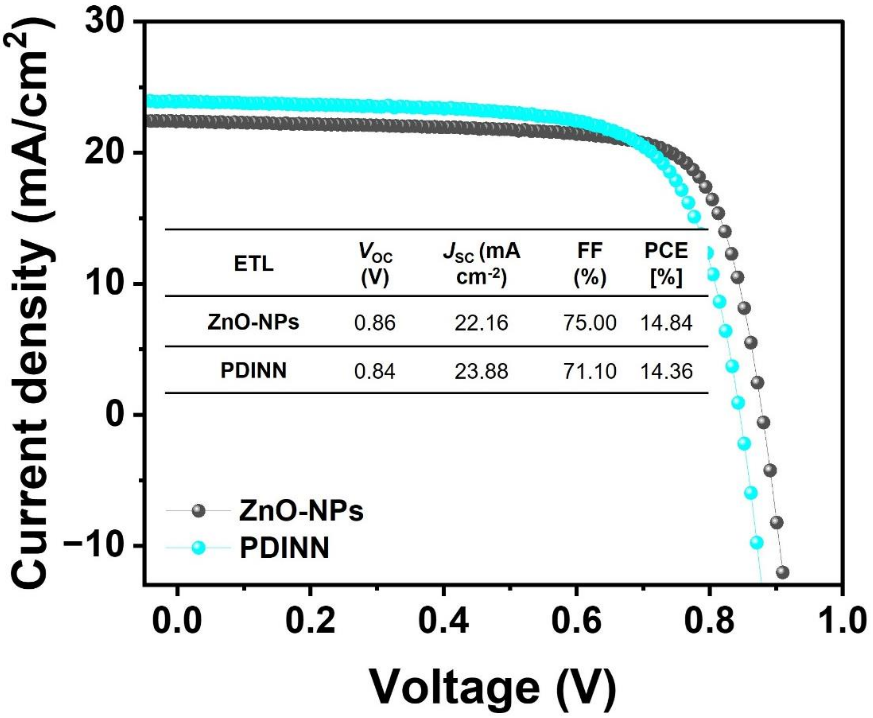

Supplementary Figure 9: J-V curves of ZnO vs PDINN

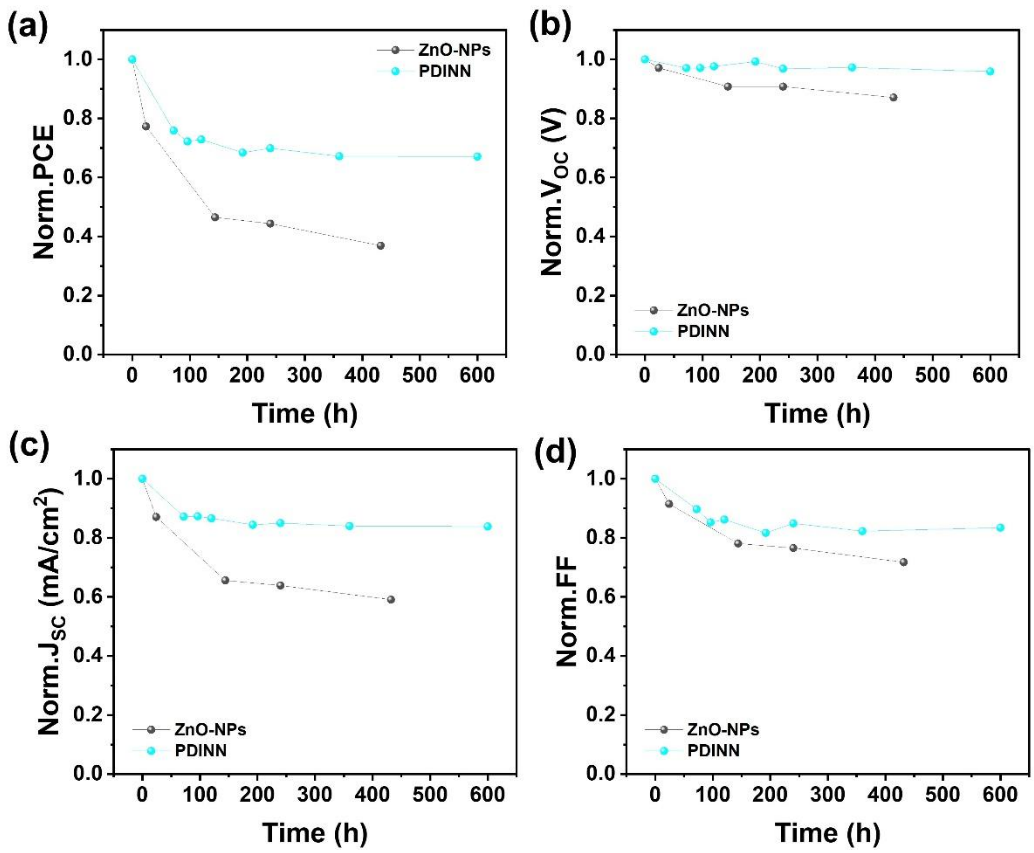

Supplementary Figure 10: The photovoltaic parameters change of device based on ZnO vs PDINN (with 2-PACz/MoOx as HTL) with encapsulation under continuous 1-sun illumination (a) PCE (b) J_{SC}, (c) V_{OC} and (d) FF.

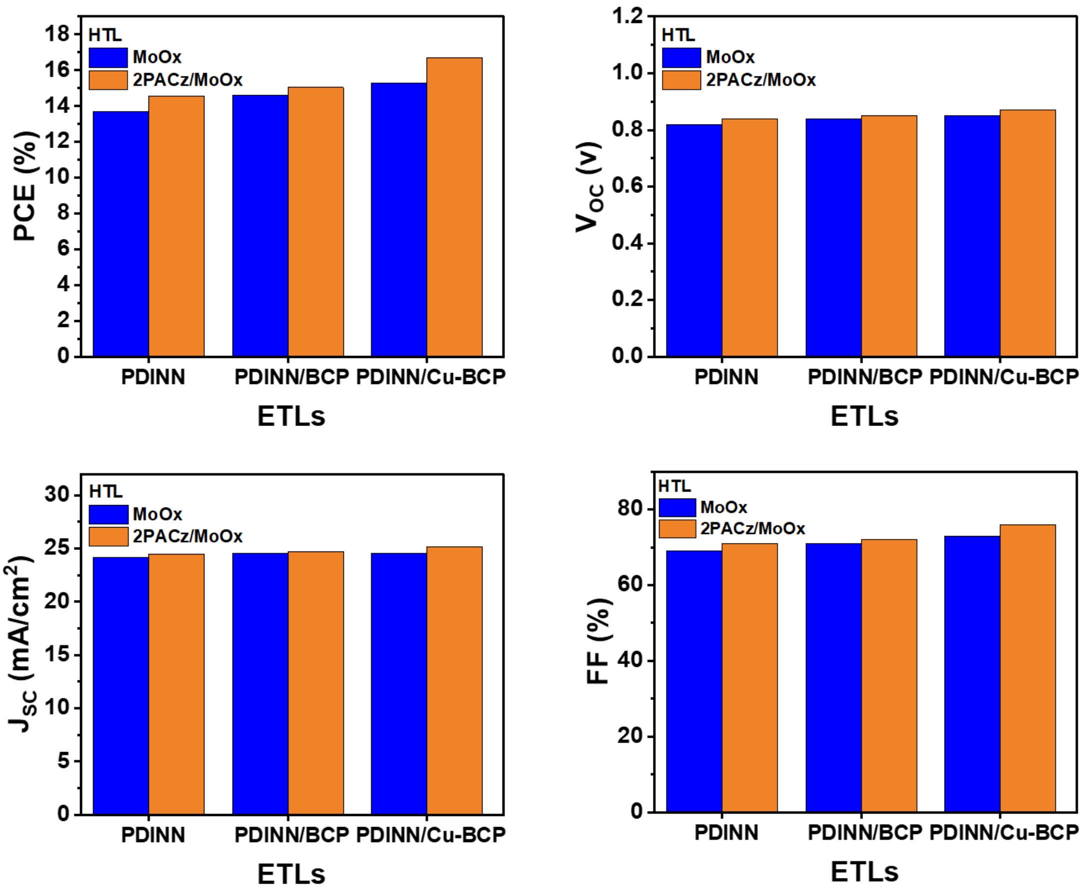

Supplementary Figure 11: Comparison of photovoltaic parameters for OSCs employing different cathode interlayers with MoOx and 2-PACz/MoOx as the anode structure.

Supplementary Table 6: Extracted charge-transfer resistance values of aged devices with different cathode interlayers (fresh devices)

ETL	R_{CT} (Ω)
PDINN	70.49
PDINN/BCP	29.85
PDINN/Cu-BCP	15.75

Supplementary Table 7: Electron mobility (μ_e) values of devices with different cathode interlayer configurations extracted from electron-only measurements.

ETL	Electron mobility ($cm^2V^{-1}\ s^{-1}$)
PDINN	4.96×10^{-3}
PDINN/BCP	6.69×10^{-3}
PDINN/Cu-BCP	7.34×10^{-3}

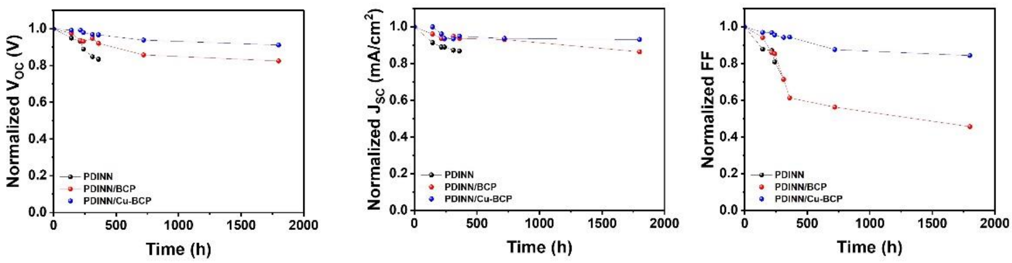

Supplementary Figure 12: Evolution of the normalized photovoltaic parameters of OSCs with different cathode interlayers during aging: (left) normalized V_{OC}, (middle) normalized J_{SC}, and (right) normalized FF during air-storage aging (25°C/25%RH) aging for PDINN, PDINN/BCP, and PDINN/Cu-BCP devices.

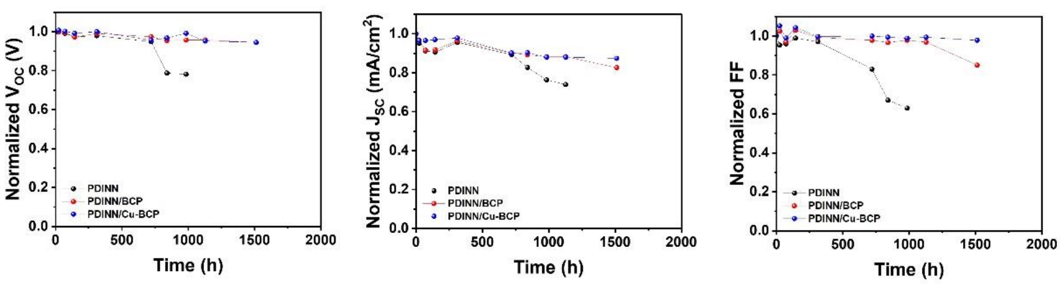

Supplementary Figure 13: Evolution of the normalized photovoltaic parameters of OSCs with different cathode interlayers during aging: (left) normalized V_{OC}, (middle) normalized J_{SC}, and (right) normalized FF during thermal humidity (65°C/65%RH) aging for PDINN, PDINN/BCP, and PDINN/Cu-BCP devices.

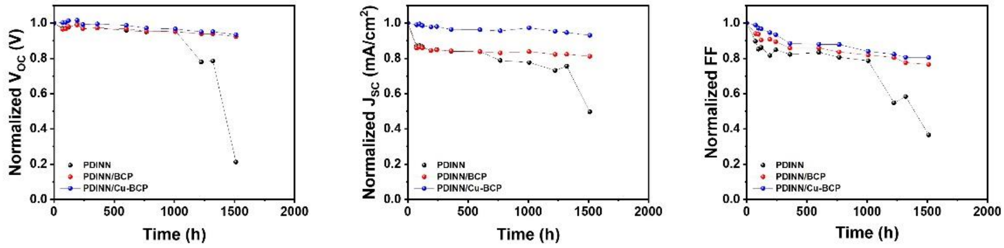

Supplementary Figure 14: Evolution of the normalized photovoltaic parameters of OSCs with different cathode interlayers during aging: (left) normalized V_{OC}, (middle) normalized J_{SC}, and (right) normalized FF during continuous 1-sun photo-illumination (25°C/25%RH) aging for PDINN, PDINN/BCP, and PDINN/Cu-BCP devices.

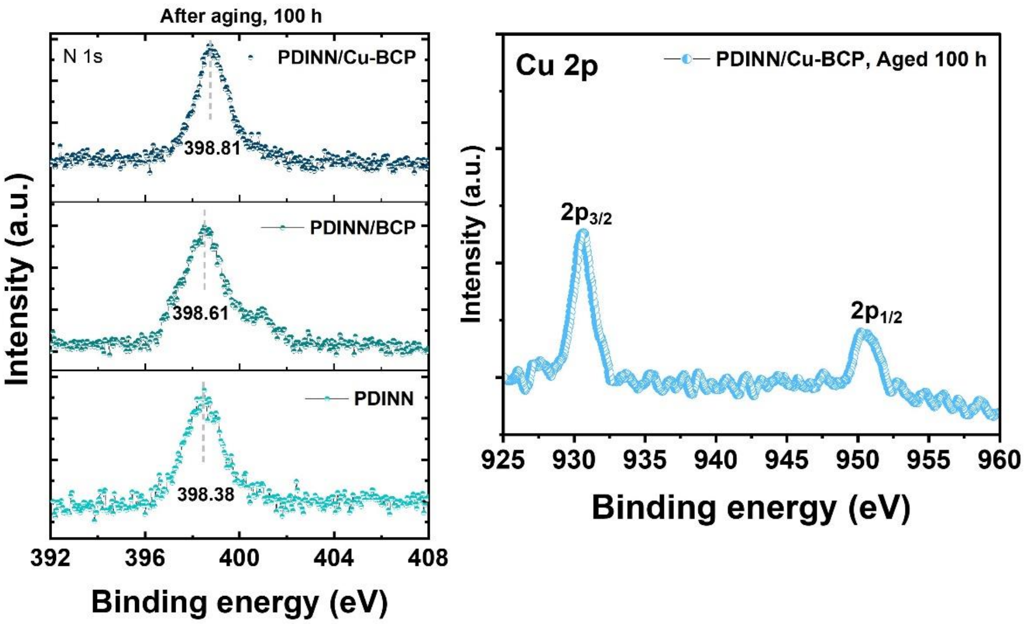

Supplementary Figure 15: XPS analysis of photo-aged cathode interlayer films after 100 h of continuous illumination. (a) High-resolution N 1s spectra of ITO/PDINN, ITO/PDINN/BCP, and ITO/PDINN/Cu-BCP. (b) High-resolution Cu 2p spectrum of ITO/PDINN/Cu-BCP after photo-aging.

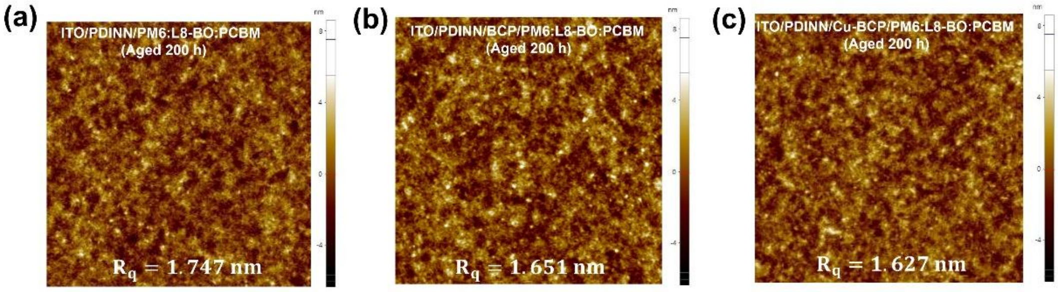

Supplementary Figure 16: AFM of various CIL/photoactive layer after 200 h under thermal-humidity aging (65°C/65% RH)

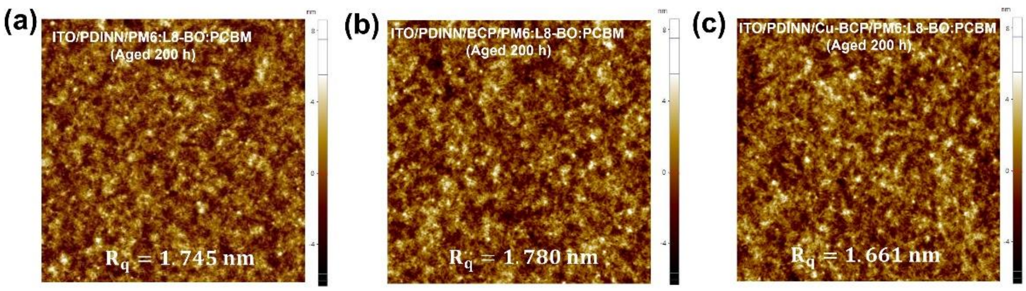

Supplementary Figure 17: AFM of various CIL/photoactive layer after 200 h under continuous illumination (1-sun)

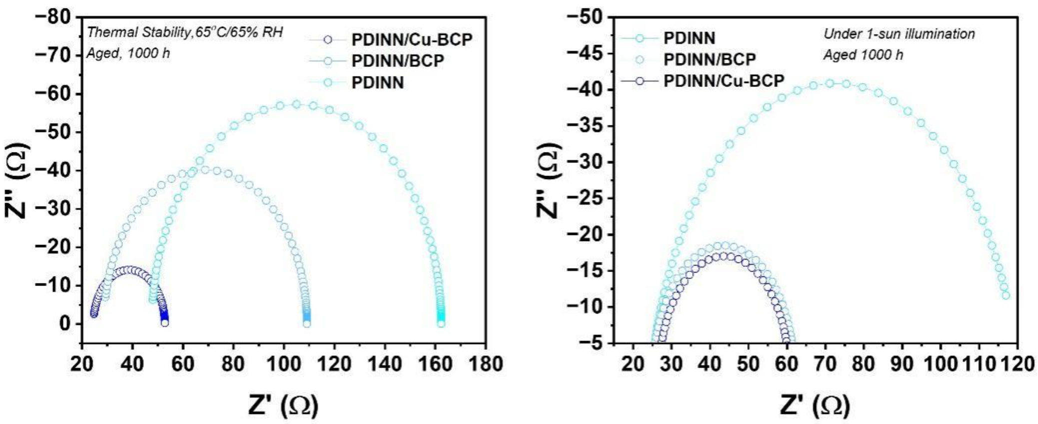

Supplementary Figure 18: EIS analysis of aged OSCs with different cathode interlayers. Left: Nyquist plots of devices aged under 65 °C/65% RH for 1000 h. Right: Nyquist plots of devices aged under continuous 1 sun illumination for 1000 h

Supplementary Table 8: Extracted charge-transfer resistance values of aged devices with different cathode interlayers under thermal-humidity and photostability tests.

ETL	**R_{CT} (Ω), 65 °C/65% RH, 1000 h**	**R_{CT} (Ω), 1-sun illumination, 1000 h**
PDINN	114.60	95.84
PDINN/BCP	80.47	39.68
PDINN/Cu-BCP	29.30	34.07